PHILOSOPHICAL TRANSACTIONS OF THE ROYAL SOCIETY A MATHEMATICAL, PHYSICAL & ENGINEERING SCIENCES

Wavelets in time-series analysis

Guy P. Nason and Rainer von Sachs

Phil. Trans. R. Soc. Lond. A 1999 **357**, 2511-2526
doi: 10.1098/rsta.1999.0445

THE ROYAL SOCIETY

Wavelets in time-series analysis

By Guy P. Nason[1] and Rainer von Sachs[2]

[1]*Department of Mathematics, University of Bristol, University Walk, Bristol BS8 1TW, UK*
[2]*Institute of Statistics, Catholic University of Louvain, Louvain-la-Neuve, Belgium*

This article reviews the role of wavelets in statistical time-series analysis. We survey work that emphasizes scale, such as estimation of variance, and the scale exponent of processes with a specific scale behaviour, such as $1/f$ processes. We present some of our own work on locally stationary wavelet (LSW) processes, which model both stationary and some kinds of non-stationary processes. Analysis of time-series assuming the LSW model permits identification of an evolutionary wavelet spectrum (EWS) that quantifies the variation in a time-series over a particular scale and at a particular time. We address estimation of the EWS and show how our methodology reveals phenomena of interest in an infant electrocardiogram series.

Keywords: Allan variance; locally stationary time-series; long-memory processes; time-scale analysis; wavelet processes; wavelet spectrum

1. Introduction

Reviewing the role of wavelets in statistical time-series analysis (TSA) appears to be quite an impossible task. For one thing, wavelets have become so popular that such a review could never be exhaustive. Another, more pertinent, reason is that there is no such thing as *one* statistical time-series *analysis*, as the very many different fields encompassed by TSA are, in fact, so different that the choice of a particular methodology must naturally vary from area to area. Examples for this are numerous: think about the fundamentally different goals of treating comparatively short correlated biomedical time-series to explain, for example, the impact of a set of explanatory variables on a response variable, or of analysing huge inhomogeneous datasets in sound, speech or electrical engineering, or, finally, building models for a better understanding and possibly prediction of financial time-series data.

Hence, here we can only touch upon some aspects of where and why it can be advantageous to use wavelet methods in some areas of statistical TSA. We consider the common situation where the trend and (co-)variation of autocorrelated data are to be modelled and estimated. Classically, the time-series data are assumed to be *stationary*: their characterizing quantities behave homogeneously over time. Later in this paper, we shall consider situations where some controlled deviation from stationarity is allowed.

We stress that this article does not provide an exhaustive review of this area. In particular, we shall not go into detail concerning the time-series aspects of wavelet denoising, nor the role of wavelets in *deterministic* time-series, but briefly summarize these next. Later on, we shall concentrate on seeing how wavelets can provide

information about the *scale* behaviour of a series: i.e. what is happening at different scales in the series. This type of analysis, as opposed to a frequency analysis, can be appropriate for certain types of time-series as well as provide interpretable and insightful information that is easy to convey to the non-specialist.

Wavelet denoising. Silverman (this issue) and Johnstone (this issue) describe the method and rationale behind *wavelet shrinkage*, a general technique for curve denoising problems. The specific connection with the analysis of correlated time-series data $\{Y_t\}$ is that in a general regression-like model,

$$Y_t = m(X_t) + \sigma(X_t)\epsilon_t, \quad t = 1, \ldots, T,$$

non-parametric estimation of the trend function m and/or the function σ, which measures the variability of the data, can be performed in exactly the same framework of nonlinear wavelet shrinkage as for the original simple situation of Gaussian i.i.d. data (see Silverman, this issue). In typical biomedical applications, the errors (and, hence, the Y_t themselves) need be neither uncorrelated nor even stationary (for one example, in the case of a deterministic equidistant design, $\{X_t\} = \{t/T\}$ (see von Sachs & MacGibbon 1998)). In financial time-series analysis, where the choice of $\{X_t\} = \{(Y_{t-1}, \ldots, Y_{t-p})\}$ leads to a non-parametric autoregressive model (of order p), the task is estimation of a conditional mean and variance under the assumption of *heteroscedastic* stationary errors (see, for example, Hoffmann (1999) for the case $p = 1$). Both examples, but particularly the second one, call for *localized* methods of estimation. Problems of this sort typically show regimes of comparatively smooth behaviour, which, from time to time, may be disrupted by break points or other discontinuities. A subordinate task would then be to detect and estimate the precise location of these break points, and here wavelet methods again prove useful. Finally, for this little review, we mention that wavelet shrinkage can be used for the estimation of spectral densities of stationary time-series (Neumann 1996; Gao 1997) and of time-varying spectra using localized periodogram-based estimators (von Sachs & Schneider 1996; Neumann & von Sachs 1997).

Deterministic time-series. A completely different use of wavelets in statistical time-series analysis was motivated by how wavelets originally entered the field of (deterministic) time–frequency analysis (see, for example, Rioul & Vetterli 1991; or Flandrin 1998). Here, wavelets, being *time-scale* representation methods, deliver a tool complementary to both classical and localized (e.g. windowed) Fourier analyses. We will focus next on this aspect for *stochastic* signals.

Stochastic time-series. Recently, the search for localized time-scale representations of stochastic correlated signals led to both analysing and synthesizing (i.e. modelling) mainly *non-stationary* processes with wavelets or wavelet-like bases. By non-stationarity we mean here two different types of deviation from stationarity: first, but not foremost, we will address, in § 2, wavelet analyses of certain long-memory processes that show a specific (global or local) scale behaviour, including the well-known $1/f$ (or power law) processes. However, our main emphasis is on signals with a possibly time-changing probability distribution or characterizing quantities. Overall,

from the modelling point of view, wavelets offer clear advantages mainly for the two types of non-stationary data mentioned above.

Statistical time-scale analysis performs a statistical wavelet *spectral analysis* of time-series analogous to the classical *Fourier* spectral analysis, where the *second-order* structure of the series such as variance, autocovariance (dependence structure within the series) and spectral densities are to be estimated (see Priestley 1981). The analyses depend fundamentally on processes possessing a representation in terms of random coefficients with respect to some localizing basis: in classical spectral analysis, the Fourier basis, which is perfectly localized in frequency; in time-scale analysis, a basis that is localized in time and scale. Then, the respective second-order quantities of interest (e.g. variance or autocovariance) can be represented by a superposition of the (Fourier or the wavelet) spectra. Our specific model, in § 3 *b*, uses a particular set of basis functions: discrete non-decimated wavelets.

However, before turning to scale- *and* time-localized models, the next section reviews the basic ideas about using wavelets for the *analysis* of statistical phenomena with characteristic behaviour living on certain global scales. For example, a variance decomposition on a scale-by-scale basis has considerable appeal to scientists who think about physical phenomena in terms of variation operating over a range of different scales (a classical example being $1/f$ processes). We will review a very simple example to demonstrate how insights from *analysis* can be used to derive models for the *synthesis* of stochastic processes.

Both in analysis and synthesis it is, of course, possible to *localize* these scale-specific phenomena in time as well. For the specific example of $1/f$ processes, we refer to Gonçalvès & Flandrin (1993) and more recent work of, for example, Wang *et al*. (1997), and the overview on wavelet analysis, estimation and synthesis of scaling data by Abry *et al*. (1999). The common paradigm of all these approaches is the separation of the scale on which the process data are sampled from the scale(s) where the respective behaviour is observed.

2. Estimation of 'global' scale behaviour

This section gives examples on estimating the scale characteristics of processes that do not show a location dependency. In fact, we restrict our discussion to the utility of wavelets for the analysis and synthesis of long-memory processes. We begin with a brief introduction to scalograms using the example of the *Allan variance*, originally developed by Allan (1966) as a time-domain measure of frequency stability in high-frequency oscillators (McCoy & Walden 1996). Then we turn, more specifically, to the problem of estimation of the scale exponent of $1/f$ processes, in the specific case of fractional Brownian motion (fBm).

(*a*) *Long-memory processes, Allan and wavelet variance*

For pedagogical reasons, we will concentrate on Percival & Guttorp (1994), one of the earlier papers in the vast literature in this field, and also, for a simple exposition, we will only concentrate on the Haar wavelet although other wavelets may be equally, if not more, useful.

Consider a stretch of length T of a given zero mean stochastic process $\{X_t\}_{t\in Z}$. The *Allan variance* $\sigma_X^2(\tau)$ at a particular scale $\tau \in Z$ is a measure of how averages,

over windows of length τ, change from one period to the next. If

$$\bar{X}_t(\tau) = \frac{1}{\tau}\sum_{n=0}^{\tau-1} X_{t-n},$$

then

$$\sigma_X^2(\tau) := \tfrac{1}{2}E(|\bar{X}_t(\tau) - \bar{X}_{t-\tau}(\tau)|^2). \tag{2.1}$$

In order to have a meaningful quantity independent of time t, X_t must be stationary, or at least have stationary increments of order 1.

In fact, the Allan variance turns out to be proportional to the Haar wavelet variance, another 'scale variance' based on the standard discrete Haar wavelet transform as follows. Let $\{\hat{d}_{jk}\}$ denote the (empirical) wavelet coefficients of the signal $\{X_t\}_{t=0,\ldots,T-1}$, where we deviate from standard notation in that our scales $j = -1, \ldots, -\log_2(T)$ become more negative the coarser the level of the transform, and, hence, the location index k runs from 0 to $T/2^{-j} - 1$. This proportionality can easily be observed by writing the Haar coefficients as successive averages of the data with filters $1/\sqrt{2}$ and $-1/\sqrt{2}$ (which are the high-pass filter coefficients $\{g_k\}$ of the Haar transform (see Silverman, this issue)). For example, for $j = -1$ at scale $\tau_j = 2^{-j-1} = 1$,

$$\hat{d}_{-1,k} = (1/\sqrt{2})(X_{2k+1} - X_{2k}), \quad k = 0, \ldots, T/2 - 1, \tag{2.2}$$

and it is easy to see that $\mathrm{var}\{\hat{d}_{-1,k}\} = \sigma_X^2(1)$. More generally,

$$\mathrm{var}\{\hat{d}_{jk}\} = E\hat{d}_{jk}^2 = \tau_j \sigma_X^2(\tau_j). \tag{2.3}$$

Motivated by this last equation, an unbiased estimator for the Allan variance, the so-called 'non-overlapped' estimator, is the appropriately normalized sum of the squared wavelet coefficients:

$$\hat{\sigma}_X^2(\tau_j) := \frac{2}{T}\sum_{k=0}^{T/2^{-j}-1} \hat{d}_{jk}^2. \tag{2.4}$$

This estimator has the property that each datapoint X_t contributes to exactly one coefficient $\hat{d}_{jk}$. Again only considering the finest scale, $j = -1$, formula (2.4) can be written in terms of the data as

$$\hat{\sigma}_X^2(1) = \frac{1}{T}\sum_{k=0}^{T/2-1} (X_{2k+1} - X_{2k})^2.$$

We observe immediately that one can improve upon the above estimator by summing over not just $T/2$ values of these time-series differences but over all $T-1$ possible ones. The resulting estimator will clearly have a smaller variance and also possesses independence with respect to the choice of the origin of the series $\{X_t\}$. This 'maximal-overlap' estimator, denoted by $\tilde{\sigma}_X^2(\tau_j)$, is based on the 'non-decimated' (Haar) wavelet transform (NDWT), with wavelet coefficients $\tilde{d}_{jk}$ (see the appendix for a description). The NDWT amounts to a uniform sampling in k instead of the inclusion of subsampling or decimation in each step of the standard discrete (decimated) wavelet transform (DWT).

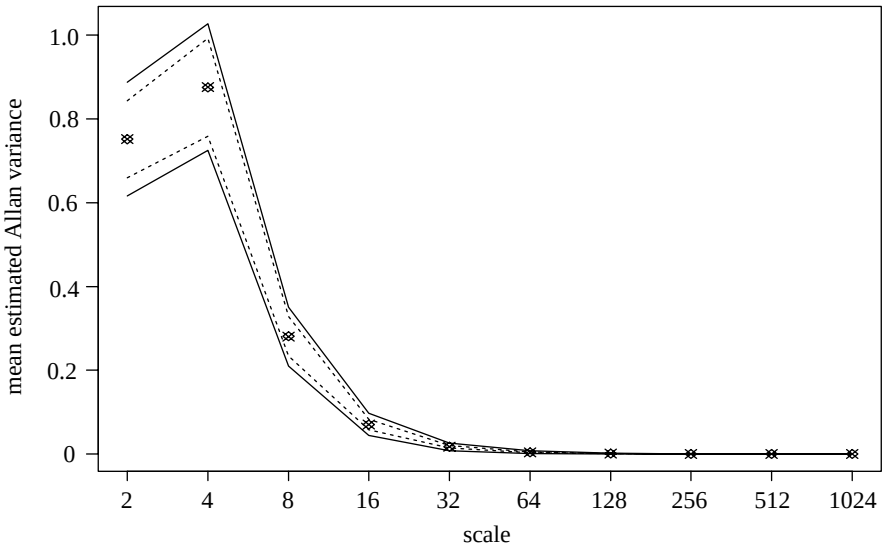

Figure 1. Mean of estimated Allan variances over 1000 simulations of the MA(3) process computed using Haar wavelet variances (see text). The mean of the estimates is shown by the symbols, the mean plus or minus twice the standard deviation of the estimate is shown by lines. For the 'non-overlap' estimator the symbols are $\times$ with solid error lines; for the 'maximal-overlap' estimator the symbols are $\diamond$ and the error lines are dotted. The theoretical values of the Allan variance at scales 2, 4 and 8 are $\frac{3}{4}$, $\frac{7}{8}$ and $\frac{36}{128}$ respectively.

Figure 1 shows an estimator for the Allan variance of the MA(3) process

$$X_t^{(2)} = \tfrac{1}{2}(\varepsilon_t + \varepsilon_{t-1} - \varepsilon_{t-2} - \varepsilon_{t-3}),$$

with standard Gaussian white noise ε_t, using both the 'non-overlap' and 'maximal-overlap' estimators. This MA process is one of a class that we will meet in § 3. The figure was produced by simulating 1024 observations from the process and computing the estimated Allan variance. This simulation procedure was repeated 1000 times and the figure actually shows the mean of all the estimated Allan variances with lines showing the accuracy of the estimates. It is clear that the 'maximal-overlap' estimator has a smaller variance for a wide range of scales τ_j. It is clear from the formula of the MA(3) process that it 'operates' over scale 4, and, thus, the Allan variance at scale 4 ($j = -2$) is largest in figure 1. Further, the Allan variance indicates that there is variation at scale 2; this is not surprising because the process formula clearly links quantities over that scale as well. However, at scale 8 and larger scales, the process has insignificant variation, and so the Allan variance decays for large scales. Using (2.3) and the orthogonality of the DWT, it is easy to see that the Allan variance for standard white noise is

$$\sigma^2(\tau_j) = 1/\tau_j = 2^{j+1}, \quad j < 0.$$

More general wavelets could be used in place of Haar in the wavelet variance estimators given above. In any case, the use of the NDWT will be beneficial as is clear from the example above.

Why is the concept of a 'scale variance' useful at all? The 'scale variance' permits a new decomposition of the process variance which is different (but related) to the

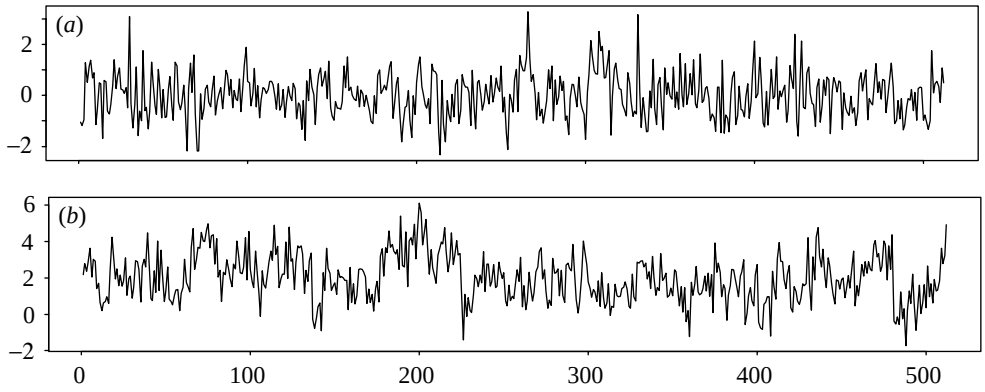

Figure 2. (*a*) Realization of an fGn process with very little 'long memory'. (*b*) Realization of an fGn process with evident long memory. In (*b*) you can 'see' a 'slow oscillation' underlying the process.

classical spectral decomposition using the (Fourier) spectral density. That is, suppose we have a stationary process $\{X_t\}$, then we can decompose its total variance $\mathrm{var}\{X_t\}$ into quantities that measure the fluctuation separately scale by scale:

$$\mathrm{var}\{X_t\} = \frac{1}{2}\sum_{j=-\infty}^{-1} \sigma_X^2(\tau_j) = \sum_j \mathrm{var}\{\tilde{d}_{jk}\}/2\tau_j. \tag{2.5}$$

Here, on the right-hand side, the scale-dependent quantities play the role of a 'wavelet spectrum' $S_j := \mathrm{var}\{\tilde{d}_{jk}\}/2\tau_j$, which, in the stationary case, is independent of time k. For white noise, $S_j = 2^j$. We will define a time-dependent wavelet spectrum in (3.4) for more general non-stationary processes in § 3.

The Allan (or wavelet) variance is of additional interest for the study of long-memory processes. These are processes in which the autocorrelation of the process decays at a very slow rate, such that it is possible for effects to persist over long time-scales (see Beran 1994). Consider a 'fractional Gaussian noise' (fGn) process with self-similarity parameter $\frac{1}{2} < H < 1$, or, more precisely, the first-order increments $\{Y_t\}$ of an fBm $B = B_H$ (with $B_0 = 0$). This process is characterized by having normally distributed stationary and self-similar increments

$$Y_t := \frac{B_{s+t} - B_s}{t} \sim \frac{B_t - B_0}{t} \sim |t|^{H-1} B_1 \sim N(0, \sigma^2 |t|^{2H-2})$$

(see, for example, Abry *et al.* 1995). Figure 2 shows sample paths for two different simulated fGn processes. Try and guess which one has the long-memory before you study the caption!

It can be shown that the Allan variance of $\{Y_t\}$ follows a power law, i.e.

$$\sigma_Y^2(\tau) = L(\tau)|\tau|^{2H-2} \quad |\tau| \gg t_0,$$

where $L(\cdot)$ is a slowly varying function for $\tau \to \infty$. Hence, a plot of $\log\{\sigma_Y^2(\tau)\}$ versus $\log(\tau)$ (or, more precisely, a least-squares or maximum-likelihood estimate of this log-linear relationship based on one of the estimators for σ_Y^2) can reveal an estimator of the parameter H, and, in general, for large enough τ one can observe to a good approximation a line with slope $2H-2$. Here we now see that it can be useful

to use wavelets other than Haar when investigating a potential relationship because different wavelets cover slightly different frequency ranges and possess differing phase behaviour.

Some example applications can be found in Percival & Guttorp (1994) on the analysis of the scales of variation within vertical ocean shear measurements, which obey a power-law process over certain ranges. Serroukh *et al*. (1998) investigate the wavelet variance of the surface albedo of pack ice, which happens to be a strongly non-Gaussian series. This paper also derives statistical properties of the estimators used for obtaining confidence intervals.

(*b*) *Wavelet spectral analysis of* $1/f$ *processes*

We now slightly change our point of view, and instead of variances over certain scales we now examine the more general quantity: the spectral density or spectrum. The spectrum is the Fourier transform of the autocovariance function of a stationary process. For its proper definition in case of the (non-stationary) fBm, we again must use the fGn, which has a power-law spectral density as follows,

$$f_Y(\omega) = L_f(\omega)|\omega|^{1-2H}, \quad 0 < |\omega| \ll t_0^{-1},$$

where, again, $L_f(\cdot)$ is a slowly varying function, now for $\omega \to 0$. If $H > \frac{1}{2}$, we observe a singularity in zero frequency that is, again, an indicator for a strongly correlated time-series, i.e. one with long memory.

As before, from the statistical point of view, there is a linear relation between $\log\{f_Y(\omega)\}$ and $\log(|\omega|)$ for small enough $|\omega|$, which allows us to base an estimator for the spectral exponent $\alpha = 1 - 2H$ on an estimator for the spectrum f_Y. This will, in fact, be one of the estimators $\hat{\sigma}_Y^2$ or $\tilde{\sigma}_Y^2$ for the wavelet variance σ_Y^2, which is related to the spectrum f_Y by the equation (2.6) below. We summarize § 2 of Abry *et al*. (1995) who clarify why wavelet is superior to traditional Fourier spectral analysis for power law processes. The two methods may be compared by examining the expectation of the wavelet variance estimator, $\hat{\sigma}_Y^2(\tau_j)$, and the expectation of the average of short-time Fourier periodograms over segments of equal length of $\{Y_t\}$. The Fourier estimator is constructed in a similar way to the wavelet variance estimator, except that Gabor-like basis functions (appropriately weighted exponentials) instead of wavelets are used. In other words, the Fourier estimator is the time marginal of a particular bilinear time–frequency distribution, the *spectrogram*, which is the squared modulus of a Gabor or short-time Fourier transform. In this context, the wavelet variance estimator is the time marginal of the *scalogram*, i.e. the squared wavelet coefficients. The properties of the two estimators are different because of the way that energy is distributed over the two different configurations of atoms (Fourier, rectangular equal-area boxes centred at equispaced nodes; wavelets, the famous constant-Q tiling with centres located on the usual wavelet hierarchy).

The expectation of the time marginal of the spectrogram can be written as the convolution of the Fourier spectrum $f_Y(\omega)$ of $\{Y_t\}$ with the squared Fourier transform of the moving window. Similarly, the expectation of the time marginal of the scalogram, i.e. of $\hat{\sigma}_Y^2(\tau_j)$ (for reasons of simplicity we only refer to the inferior estimated based on the DWT), is the convolution of $f_Y(\omega)$ with the squared modulus

of the Fourier transform $\hat{\psi}_{jk}(\omega)$ of the wavelets in the DWT, i.e.

$$\sigma_Y^2(\tau_j) = E\hat{\sigma}_Y^2(\tau_j) = \frac{2}{T}\sum_k E\hat{d}_{jk}^2 = \tau_j^{-1}\int_{-\pi}^{\pi} f_Y(\omega)|\hat{\psi}_{jk}(\omega)|^2\,\mathrm{d}\omega. \tag{2.6}$$

Abry *et al*. (1995) show foremost that in a log–log relationship of equation (2.6), the bias for estimating the spectral parameter α of f_Y becomes frequency *independent* when using averaged scalograms instead of averaged spectrograms. This is a consequence of the fact that in the Fourier domain, wavelets scale multiplicatively with respect to frequency, a property that the fixed-window spectrograms do not enjoy. Further considerations in Abry *et al*. (1995), such as those pertaining to the efficiency of the estimators, support the wavelet-based approach for these processes.

Equation (2.6) also helps to further interpret the variation of the considered estimators of $\sigma_Y^2(\tau_j)$ in the example given in figure 1. As the spectrum $f_Y(\omega)$ of the MA(3) process of this example has its power concentrated near to high frequencies, and as the variance of these estimators are approximately proportional to the square of their mean, it is clear from the integral in (2.6) that this variance increases with frequency, i.e. if we go to finer scales in the plots of figure 1.

Further examples for processes with such a singular power-law behaviour near zero frequency can be found (see Flandrin 1998), e.g. in the areas of atmospheric turbulence (see, for example, Farge, this issue), hydrology, geophysical and financial data, and telecommunications traffic (Abry *et al*. 1999), to name but a few. Whitcher *et al*. (1998) detect, test and estimate time-series variance changes. Their work can identify the scale at which the change occurs. Generalizations of these kind of tests to time-varying autocovariance and spectral density for short-memory non-stationary processes can be found in von Sachs & Neumann (1998).

In § 3 we discuss ideas of how to localize both the analysis and synthesis of the global scale behaviour discussed in this section.

(*c*) *Synthesis of long-memory processes using wavelets*

In the above considerations on *analysis* of $1/f$ processes, we saw that wavelets formed a key role. In reverse, it is not surprising that they are useful also for *synthesis*, i.e. in the theory of modelling $1/f$ processes (see, again, Abry *et al*. 1999). Indeed, it is possible to, for example, simulate $1/f$ processes using wavelets (see Wornell & Oppenheim 1992). One method for simulating fGn is given by McCoy & Walden (1996) as follows:

(a) compute the variances, S_j, of the required fGn processes by integrating its spectrum over dyadic intervals $[-2^j, -2^{j-1}] \cup [2^{j-1}, 2^j]$;

(b) for each scale j, draw a sequence of 2^{-j} independent and identically distributed normal random variables d_{jk};

(c) apply the inverse DWT to the $\{d_{jk}\}$ coefficients to obtain an approximate realization of a $1/f$ process.

Figure 2 shows two realizations from fGn processes using the McCoy & Walden (1996) methodology.

3. Wavelet processes: a particular time-scale model

(a) *Local stationarity*

Suppose that we have a time-series $\{X_t\}_{t\in\mathbb{Z}}$, and that we wish to estimate the variance $\sigma_t^2 = \mathrm{var}(X_t)$ over time. If the series is stationary, then σ_t^2 will be constant and equal to σ^2 and we can use the usual sum of squared deviations from the mean estimator on a single stretch of the observed time-series $X_1, \ldots, X_T$. As more data become available (as T increases), the estimate of the variance $\hat{\sigma}^2$ improves. Alternatively, suppose that we know that the variance of the series changes at each time point t, i.e. assume that $\mathrm{var}(X_t) = \sigma_t^2$ for all $t \in \mathbb{Z}$ where none of the σ_t^2 are the same. Here the series is non-stationary and we do not have much hope in obtaining a good estimate of σ_t^2 since the *only* information we can obtain about σ_t^2 comes from the single X_t. As a third alternative, suppose the variance of a time-series changes *slowly* as a function of time t. Then the variance around a particular time t^* could be estimated by pooling information from X_t close to t^*.

A similar situation occurs if the long-memory parameter H in the previous section changes over time, i.e. $H = H(t)$, then the Allan variance would also change over time:

$$\sigma_Y^2(t,\tau) = E(|\bar{Y}_t(\tau) - \bar{Y}_{t-\tau}(\tau)|^2) \sim \tau^{2H(t)-2}.$$

For a series with such a structure, we would hopefully observe

$$\tilde{d}_{j,k}^2 \approx \tilde{d}_{j,k+1}^2,$$

for the NDWT coefficients. To estimate the Allan variance we would need to construct local averages. In other words, we would not sum over *all* empirical NDWT coefficients but would perform adaptive averaging of the $\tilde{d}_{jk}^2$ over k for fixed scale j.

Time-series whose statistical properties are slowly varying over time are called *locally stationary*. Loosely speaking, if you examine them at close range they appear to be stationary and if you can collect enough data in their region of local stationarity then you can obtain sensible estimates for their statistical properties, such as variance (or autocovariance or the frequency spectrum).

One possibility for modelling time-series such as these is to *assume* that

$$\mathrm{var}(\tilde{d}_{j,k}) \approx \mathrm{var}(\tilde{d}_{j,k+1}), \tag{3.1}$$

so that we have some chance of identifying/estimating coefficients from one realization of a time-series. More generally, an early idea for 'local stationarity', due to Silverman (1957), proposes

$$\mathrm{cov}(X_t, X_s) = c(t,s) \approx m(\tfrac{1}{2}(s+t))\gamma(s-t) := m(k)\gamma(\tau), \tag{3.2}$$

where $k = \frac{1}{2}(s+t)$ and $\tau = t-s$. This model says that the covariance behaves locally as a typical stationary autocovariance but then varies from place to place depending on k. The Silverman model reflects our own wavelet-specific model given in (3.5) except that ours decomposes γ over scales using a wavelet-like basis. Other early important work in this area can be found in Page (1952) and Priestley (1965). More recently, Dahlhaus (1997) introduced an interesting model that poses estimation of time-series statistical properties (such as variance) as a curve estimation problem (which bestows great advantages when considering the performance of estimators because it assumes a *unique* spectrum).

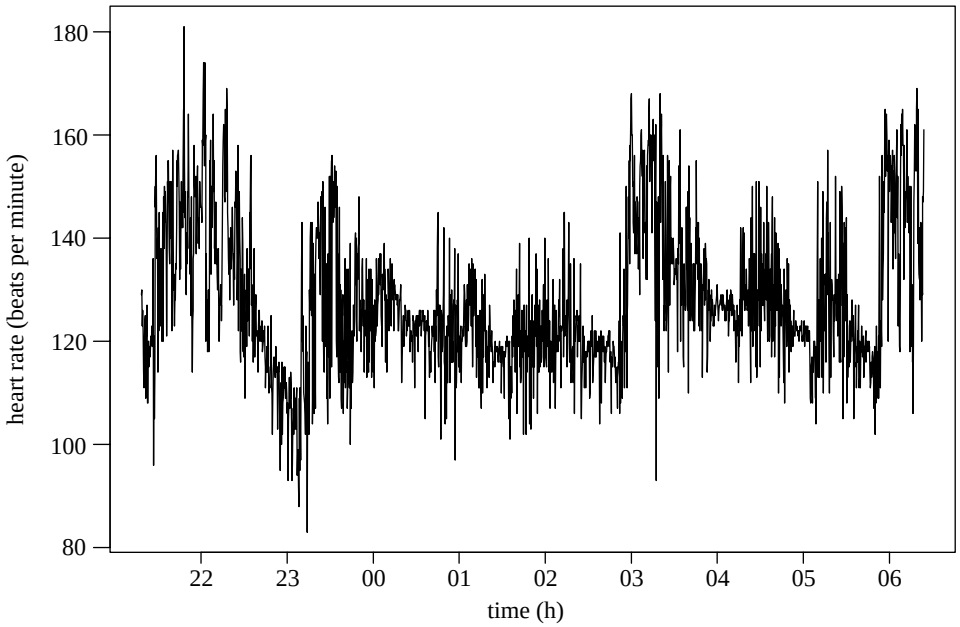

Figure 3. ECG recording of a 66-day-old infant. Series is sampled at $\frac{1}{16}$ Hz and is recorded from 21:17:59 to 06:27:18. There are $T = 2048$ observations.

Figure 3 shows an example of a time-series that is not stationary. It shows the electrocardiogram (ECG) recording of a 66-day-old infant. There are a number of interesting scientific and medical issues concerning such ECG data, e.g. building and interpreting models between ECG and other covariates such as infant sleep state (see Nason *et al*. 1999). However, for the purposes of this article, we shall confine ourselves to examining how the variance of the series changes as a function of time and scale. Further analyses of this sort can be found in Nason *et al*. (1998).

(*b*) *Locally stationary wavelet processes*

(i) *The processes model*

A time-domain model for encapsulating localized scale activity was proposed by Nason *et al*. (1999). They define the *locally stationary wavelet* (LSW) process by

$$X_t = \sum_{j=-J}^{-1} \sum_{k \in \mathbb{Z}} w_{j,k} \psi_{jk}(t) \xi_{jk}, \quad \text{for } t = 0, \ldots, T-1, \tag{3.3}$$

where the $\{\xi_{jk}\}$ are mutually orthogonal zero mean random variables, the $\psi_{jk}(t)$ are discrete non-decimated wavelets (as described in the appendix), and the $w_{j,k}$ are amplitudes that quantify the energy contribution to the process at scales j and location k. Informally, the process X_t is built out of *wavelets with random amplitudes*. The LSW construction is similar in some ways to the well-known construction of stationary processes out of sinusoids with random amplitudes.

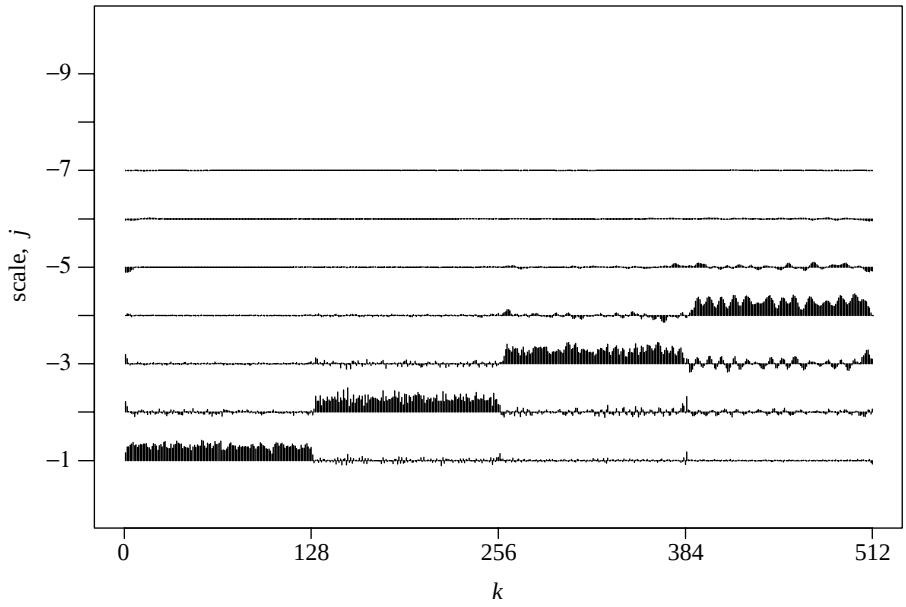

Figure 4. EWS estimate using non-decimated Haar wavelet transform. (Simulation generated) plot showing (estimated) EWS for concatenated Haar process. The horizontal axis shows 'normal' time k but could be labelled in rescaled time $z = k/512$.

(ii) *Evolutionary wavelet spectrum and local variance*

To quantify how the size of $w_{j,k}$ changes over time, we embed our model (3.3) into the Dahlhaus (1997) framework. To model locally stationary processes we use our assumption (3.1) to insist that $w^2_{j,k} \approx w^2_{j,k+1}$, which forces $w^2_{j,k}$ to change slowly over k. Stationary processes can be included in this model by ensuring that $w^2_{j,k}$ is constant with respect to k. A convenient measure of the variation of $w^2_{j,k}$ is obtained by introducing rescaled time, $z \in (0, 1)$, and defining the *evolutionary wavelet spectrum* (EWS) by

$$S_j(z) = S_j(k/T) \approx w^2_{j,k}, \tag{3.4}$$

for $k = 0, \ldots, T-1$. In the stationary case we lose the dependence on z (k) and obtain the 'wavelet spectrum' or Allan variance given just after formula (2.5). One can see that as more time-series observations are collected (as T increases), one obtains more information about $S_j(z)$ on a grid of values k/T, which makes the estimation of $S_j(z)$ a standard statistical problem.

The important thing to remember about the EWS is that

$S_j(z)$ *quantifies the contribution to process variance at scale* j *and time* z.

In other words, a large value of $S_j(z)$ indicates that there is a large amount of oscillatory power operating at scale j around location z. For examples of this, see figures 4 and 5.

For a non-stationary process, we would expect the variance of the process to vary over time and so we would expect our model to exhibit a time-localized version

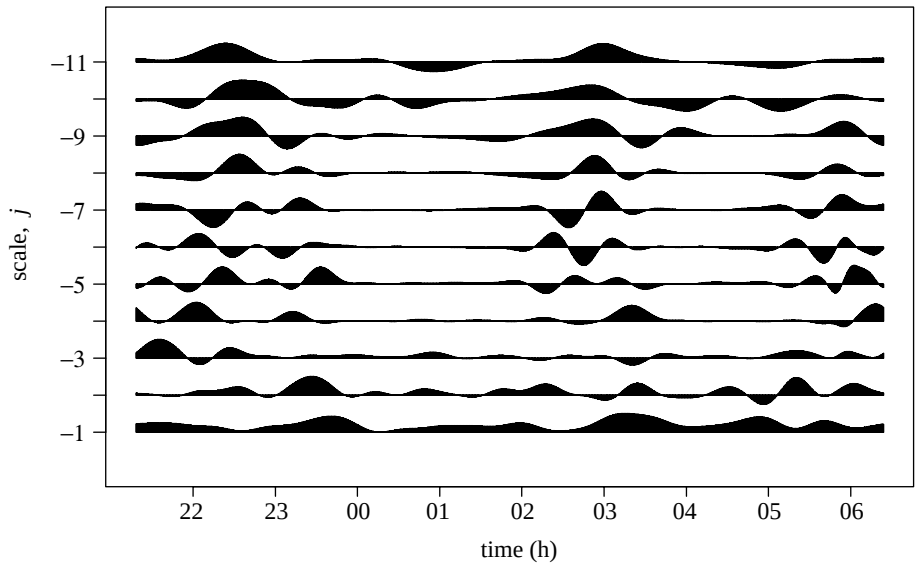

Figure 5. EWS estimate using non-decimated Haar wavelet transform. Estimate of the evolutionary spectrum $S_j(z)$ for infant ECG series shown in figure 3 (just as figure 4 shows for the simulated concatenated Haar process). The original time axis is shown although it is really rescaled time in the interval $(0, 1)$.

of (2.5), i.e. something like

$$\mathrm{var}(X_k) = \sum_j w_{j,k}^2,$$

or, more precisely, (3.7) below. If one takes our process model (3.3) and forms the autocovariance of X_t, then one (asymptotically) obtains an expression in terms of the *autocorrelation* function of the *wavelets*. Let $c(z, \tau)$ define this *localized autocovariance*,

$$\lim_{T\to\infty} \mathrm{cov}(X_{[zT]-\tau}, X_{[zT]+\tau}) = c(z,\tau) = \sum_{j=-\infty}^{-1} S_j(z)\Psi_j(\tau), \tag{3.5}$$

where $\Psi_j(\tau)$ is the autocorrelation function of the discrete non-decimated wavelets defined by (for Haar 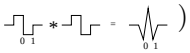)

$$\Psi_j(\tau) = \sum_{k=-\infty}^{\infty} \psi_{jk}(0)\psi_{jk}(\tau), \tag{3.6}$$

for $j < 0$. The representation in (3.3) is not unique because of the nature of the overdetermined non-decimated wavelet system. However, the autocovariance representation in (3.5) is unique. Relation (3.5) is reminiscent of the Silverman (1957) idea with $S_j(\cdot)$ playing the role of $m(\cdot)$ and $\Psi_j(\tau)$ the role of $\gamma(\tau)$, except that our model separates the behaviour over scales. Relation (3.5) also allows us to define the

localized variance at time z by

$$v(z) = c(z, 0) = \sum_{j=-\infty}^{-1} S_j(z), \tag{3.7}$$

i.e. the promised localized version of (2.5), note that $\Psi_j(0)$ is always 1 for all scales j. For stationary series, the localized autocovariance collapses to the usual autocovariance $c(\tau)$.

For estimation of the EWS we implement the idea of local averaging expressed in § 3 *a*. The EWS may be estimated by a corrected *wavelet periodogram*, which is formed by taking the NDWT coefficients, $\tilde{d}_{jk}$, of the sample realization, squaring them, and then performing a correction to disentangle the effect of the overdetermined NDWT. Like the classical periodogram (see Priestley 1981), the corrected wavelet periodogram is a noisy estimator of the EWS and needs to be smoothed to provide good estimates. The smoothing could be carried out by any number of methods, but, since we wish to be able to capture sharp changes in the EWS, we adopt wavelet shrinkage techniques (Donoho *et al*. 1995; Coifman & Donoho 1995). Figure 5 shows a smoothed corrected wavelet periodogram for the infant ECG data. For further detailed analyses on this dataset see Nason *et al*. (1998).

(iii) *Motivating example: Haar MA processes*

The MA(1) process,

$$X_t^{(1)} = (\varepsilon_t - \varepsilon_{t-1})/\sqrt{2},$$

is an LSW process as in (3.3), where the amplitudes are equal to 1 for $j = -1$ and zero otherwise, and the constructing wavelets ψ_{jk} are Haar non-decimated wavelets as given in the appendix. The autocovariance function of $X_t^{(1)}$ is $c(\tau) = 1, -\frac{1}{2}, 0$ for $\tau = 0, \pm 1$, otherwise, and this c is precisely the finest scale Haar autocorrelation wavelet $\Psi_{-1}(\tau)$. So this special Haar MA process satisfies (3.5) with $S_{-j}(z) = 0$ for all $j < -1$ and $S_{-1}(z) = 1$ (and this agrees with (3.4) since the amplitudes are 1 for $j = -1$ only, and zero otherwise). We already met the MA process $X_t^{(2)}$ in § 2 (its Allan variance was plotted in figure 1). By the same argument, its autocovariance function is, this time, the next-finest scale Haar autocorrelation wavelet $\Psi_{-2}(\tau)$. Similarly, we can continue in this way defining the rth order Haar MA$(2^r - 1)$ process $X_t^{(r)}$, which has $\Psi_{-r}(\tau)$ for its autocovariance function for integers $r > 0$. Each of the Haar MA processes is stationary, but we can construct a non-stationary process by concatenating the Haar MA processes. For example, suppose we take 128 observations from each of $X_t^{(1)}$, $X_t^{(2)}$, $X_t^{(3)}$ and $X_t^{(4)}$ and concatenate them (a realization from such a process is shown in Nason *et al*. (1998)). As a time-series of 512 observations, the process will not be stationary. The Haar MA processes have $S_{-j}(z) = 0$ for $-j \neq r$ and all z, and $S_{-r}(z) = 1$ for $z \in ([r-1]/4, r/4)$, a plot of which appears in figure 4 (remember $z = k/512$ is rescaled time).

The plot clearly shows that from time 1 to 128, the Haar MA(1) process is active with variation active at scale -1 (scale $2^{-j} = 2$), then, at time 128, the MA(1) process, $X_t^{(1)}$, changes to the MA(3) process, $X_t^{(2)}$, until time 256, and so on.

Indeed, the section from 128 to 256 ($z \in (\frac{1}{4}, \frac{1}{2})$) should be compared with figure 1, which shows the Allan variance of $X_t^{(2)}$, which would be equivalent to averaging over the 128–256 time period. However, the EWS plot above does not show any power

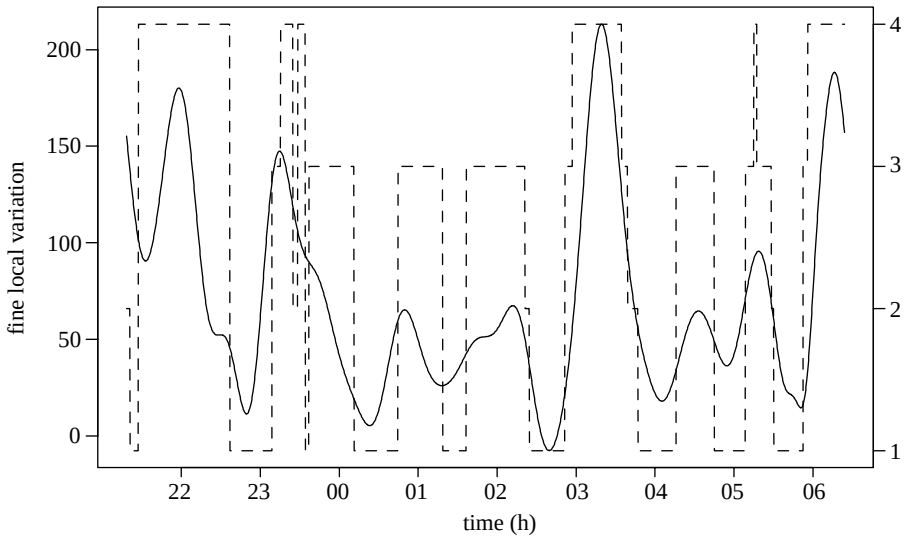

Figure 6. Estimate of local variation at fine scales for infant ECG series shown in figure 3 (solid line). The dashed line shows the sleep state of the infant (visually determined by a trained observer) ranging from 1 (quiet sleep), 2 (between 1 and 3), 3 (active sleep), 4 (awake). The original time axis is shown although z is really rescaled time in the interval $(0, 1)$.

at scales $j = -1$ ($\tau_j = 2$) and $j = -3$ ($\tau_j = 8$) unlike the Allan variance plot. The absence of power in the EWS plot is because of the disentanglement mentioned in (ii).

(iv) *Application to infant ECG*

Figure 5 shows an estimate of the evolutionary wavelet spectrum for the infant ECG data. It can be useful to aggregate information over scales. Figure 6 displays the variation in the ECG series at fine scales. The fine-scale plot was obtained by summing over contributions from scales -1 to -4 in the smoothed corrected wavelet periodogram (*ca.* 32 s, 1, 2 and 4 min time-scales). The dashed line in figure 6 shows another covariate: the sleep state of the infant as judged by a trained observer. It is clear that there is a correlation between the ECG and the sleep state that can be exploited. There is no real clear link between the sleep state and the EWS at coarse and medium scales. However, a plot of an estimate of the localized variance v (not shown here) gives some idea of overall sleep behaviour.

The EWS is a useful tool in that it provides insight into the time-scale behaviour of a time-series (much in the same way as a periodogram gives information about power in a stationary time-series at different frequencies). However, the EWS has additional uses: Nason *et al*. (1999) have also used the EWS to build models between sleep state (expensive and intrusive to measure) and ECG (cheap and easy), which allow estimates of future sleep state values to be predicted from future ECG values.

We thank P. Fleming, A. Sawczenko and J. Young of the Institute of Child Health, Royal Hospital for Sick Children, Bristol, for supplying the ECG data. G.P.N. was supported in part by EPSRC grants GR/K70236 and GR/M10229, and R.v.S. by DFG grant Sa 474/3-1 and by EPSRC Visiting Fellowship GR/L52673.

Appendix A. Discrete non-decimated wavelets

Discrete non-decimated wavelets are merely the vectors of 'filter' coefficients that appear in the matrix representation of the DWT. We shall define those that appear at scale $-j$ to be ψ_j. So, for example, with Haar

$$\psi_{-1} = \left(\frac{1}{\sqrt{2}}, -\frac{1}{\sqrt{2}}\right), \qquad \psi_{-2} = (\tfrac{1}{2}, \tfrac{1}{2}, -\tfrac{1}{2}, -\tfrac{1}{2}),$$

and so on for other scales. The ψ_j for $j = -1, \ldots, -J$ can be obtained for any Daubechies compactly supported wavelet using the formulae

$$\tilde{h}_{j-1,n} = \sum_k h_{n-2k} \tilde{h}_{j,k}, \qquad \psi_{j,n} = \sum_k g_{n-2k} \tilde{h}_{j,k},$$

where $\{h_k\}$ and $\{g_k\}$ are the usual Daubechies quadrature mirror filters, and

$$\tilde{h}_{-1,k} = h_k.$$

For non-decimated wavelets, $\psi_{jk}(\tau)$ is the kth element of the vector $\psi_{j(k-\tau)}$, i.e. ψ_{jk} shifted by integers τ. The key point for *non-decimated* discrete wavelets is that they can be shifted to any location and not just by shifts of 2^{-j} (as in the DWT). Hence, non-decimated discrete wavelets are no longer orthogonal but are an overcomplete collection of shifted vectors. The NDWT can be computed through a fast algorithm (similar to the Mallat pyramid algorithm described in Silverman, this issue), which takes a computational effort of order $n \log n$ for a dataset of length n. See Nason & Silverman (1995) for a more detailed description of the NDWT.

References

Abry, P., Gonçalvès, P. & Flandrin, P. 1995 Wavelets, spectrum analysis and $1/f$ processes. In *Wavelets and statistics* (ed. A. Antoniadis & G. Oppenheim). Springer Lecture Notes in Statistics, no. 103, pp. 15–29.

Abry, P., Flandrin, P., Taqqu, M. & Veitch, D. 1999 Wavelets for the analysis, estimation and synthesis of scaling data. In *Self similar network traffic analysis and performance evaluation* (ed. K. Park & W. Willinger). Wiley.

Allan, D. W. 1966 Statistics of atomic frequency clocks. *Proc. IEEE* **31**, 221–230.

Beran, J. 1994 *Statistics for long-memory processes*. London: Chapman and Hall.

Coifman, R. R. & Donoho, D. L. 1995 Translation-invariant denoising. In *Wavelets and statistics* (ed. A. Antoniadis & G. Oppenheim). Springer Lecture Notes in Statistics, no. 103, pp. 125–150.

Dahlhaus, R. 1997 Fitting time series models to nonstationary processes. *Ann. Statist.* **25**, 1–37.

Donoho, D. L., Johnstone, I. M., Kerkyacharian, G. & Picard, D. 1995 Wavelet shrinkage: asymptopia? (with discussion). *J. R. Statist. Soc.* B **57**, 301–369.

Flandrin, P. 1998 *Time–frequency/time-scale analysis*. Wavelet Analysis and its Applications, vol. 10. Academic.

Gao, H.-Ye. 1997 Choice of thresholds for wavelet shrinkage estimate of the spectrum. *J. Time Series Analysis* **18**, 231–251.

Gonçalvès, P. & Flandrin, P. 1993 Bilinear time-scale analysis applied to local scaling exponents estimation. In *Progress in wavelet analysis and applications* (ed. Y. Meyer & S. Roques), pp. 271–276. Gif-sur-Yvette: Editions Frontières.

Hoffmann, M. 1999 On nonparametric estimation in nonlinear AR(1)-models. *Statist. Prob. Lett.* (In the press.)

McCoy, E. J. & Walden, A. T. 1996 Wavelet analysis and synthesis of stationary long-memory processes. *J. Computational Graphical Statist.* **5**, 26–56.

Nason, G. P. & Silverman, B. W. 1995 The stationary wavelet transform and some statistical applications. In *Wavelets and statistics* (ed. A. Antoniadis & G. Oppenheim). Springer Lecture Notes in Statistics, no. 103, pp. 281–300.

Nason, G. P., von Sachs, R. & Kroisandt, G. 1998 Wavelet processes and adaptive estimation of the evolutionary wavelet spectrum. Discussion Paper 98/22, Institut de Statistique, UCL, Louvain-la-Neuve.

Nason, G. P., Sapatinas, T. & Sawczenko, A. 1999 Statistical modelling of time series using non-decimated wavelet representations. Preprint, University of Bristol.

Neumann, M. 1996 Spectral density estimation via nonlinear wavelet methods for stationary non-Gaussian time series. *J. Time Series Analysis* **17**, 601–633.

Neumann, M. & von Sachs, R. 1997 Wavelet thresholding in anisotropic function classes and application to adaptive estimation of evolutionary spectra. *Ann. Statist.* **25**, 38–76.

Page, C. H. 1952 Instantaneous power spectra. *J. Appl. Phys.* **23**, 103–106.

Percival, D. B. & Guttorp, P. 1994 Long-memory processes, the Allan variance and wavelets. In *Wavelets in geophysics* (ed. E. Foufoula-Georgiou & P. Kumar), pp. 325–344. Academic.

Priestley, M. B. 1965 Evolutionary spectra and non-stationary processes. *J. R. Statist. Soc.* B **27**, 204–237.

Priestley, M. B. 1981 *Spectral analysis and time series*. Academic.

Rioul, O. & Vetterli, M. 1991 Wavelets and signal processing. *IEEE Sig. Proc. Mag.* **8**, 14–38.

Serroukh, A., Walden, A. T. & Percival, D. B. 1998 Statistical properties of the wavelet variance estimator for non-Gaussian/non-linear time series. Statistics Section Technical Report, TR-98-03. Department of Mathematics, Imperial College, London.

Silverman, R. A. 1957 Locally stationary random processes. *IRE Trans. Inform. Theory* **IT-3**, 182–187.

von Sachs, R. & MacGibbon, B. 1999 Nonparametric curve estimation by wavelet thresholding with locally stationary errors. (Submitted.)

von Sachs, R. & Neumann, M. 1999 A wavelet-based test for stationarity. (Submitted.)

von Sachs, R. & Schneider, K. 1996 Wavelet smoothing of evolutionary spectra by non-linear thresholding. *Appl. Comp. Harmonic Analysis* **3**, 268–282.

Wang, Y., Cavanaugh, J. & Song, Ch. 1997 Self-similarity index estimation via wavelets for locally self-similar processes. Preprint, Department of Statistics, University of Missouri.

Whitcher, B., Byers, S. D., Guttorp, P. & Percival, D. B. 1998 Testing for homogeneity of variance in time series: long memory, wavelets and the Nile river. (Submitted.)

Wornell, G. W. & Oppenheim, A. V. 1992 Estimation of fractal signals from noisy measurements using wavelets. *IEEE Trans. Sig. Proc.* **40**, 611–623.

PHILOSOPHICAL TRANSACTIONS OF THE ROYAL SOCIETY A MATHEMATICAL, PHYSICAL & ENGINEERING SCIENCES